

Search for pair production of Higgs bosons
in the $b\bar{b}b\bar{b}$ final state using proton–proton
collisions at $\sqrt{s} = 13$ TeV with the ATLAS
detector

A DISSERTATION PRESENTED
BY
BAOJIA TONG
TO
THE DEPARTMENT OF PHYSICS

IN PARTIAL FULFILLMENT OF THE REQUIREMENTS
FOR THE DEGREE OF
DOCTOR OF PHILOSOPHY
IN THE SUBJECT OF
PHYSICS

HARVARD UNIVERSITY
CAMBRIDGE, MASSACHUSETTS
MAY 2018

©2017-2018 – BAOJIA TONG
ALL RIGHTS RESERVED.

Search for pair production of Higgs bosons in the $b\bar{b}b\bar{b}$ final state using proton–proton collisions at $\sqrt{s} = 13$ TeV with the ATLAS detector

ABSTRACT

We present a search for Higgs boson pair production, with the $b\bar{b}b\bar{b}$ final state. This analysis uses the full 2015 and 2016 data collected by the ATLAS Collaboration at $\sqrt{s} = 13$ TeV, corresponding to $3.2 \pm 0.2 \text{ fb}^{-1}$ of 2015 and $32.9 \pm 1.1 \text{ fb}^{-1}$ of 2016 pp collision data. Improvements with respect to the previous analysis are mainly in the boosted regime, where the resonance signal is between 2500 GeV and 3000 GeV. The data is found to be compatible with the Standard model, and no signs of new physics have been observed. The results are interpreted in the context of the bulk Randall-Sundrum warped extra dimension model with a Kaluza-Klein graviton decaying to hh , with the coupling k/\bar{M}_{Pl} , chosen to be in the allowed range 1.0 – 2.0. The results are also interpreted with the Type 2 two-Higgs doublet model (2HDM) where the neutral heavy CP-even H scalar decays to hh .

Contents

0	INTRODUCTION	1
1	MOTIVATION AND THEORY	5
1.1	The Standard Model and the Higgs Boson	5
1.2	Standard Model di-Higgs production	7
1.3	Beyond the Standard Model Physics di-Higgs production	8
1.4	Di-Higgs Decay	12
1.5	LHC previous search results	12
2	CONCLUSION	13
	REFERENCES	15

Listing of figures

1.1	Fermions and bosons of the Standard Model and their properties ¹ , where all the values are measured experimentally.	6
1.2	Feynman diagrams contributing to di-Higgs production via gluon-gluon fusion, through the Higgs-fermion Yukawa interactions 1.2a the Higgs boson self-coupling 1.2b, at leading order. Only Figure 1.2b probes λ_{hhh}	7
1.3	Total cross sections (y-axis) at the NLO in QCD for the six largest di-Higgs production channels at p-p colliders at different energy (x-axis). The thickness of the lines corresponds to the scale and PDF uncertainties added linearly. H refers to the SM Higgs.	8
1.4	BSM Higgs boson pair production: non-resonant production proceeds through changes in the SM Higgs couplings in 1.4a and 1.4b, resonant production proceeds through 1.4c an intermediate resonance, X . H and h both refers to the SM Higgs.	9
1.5	Total cross sections (y-axis) at the LO and NLO in QCD for di-Higgs production channels, at the $\sqrt{s} = 14$ TeV LHC as a function of the self-interaction coupling λ (x-axis) . The dashed (solid) lines and light- (dark-) colour bands correspond to the LO (NLO) results and to the scale and PDF uncertainties added linearly. The SM values of the cross sections are obtained at $\frac{\lambda}{\lambda_{SM}} = 1$. H refers to the SM Higgs.	10

Listing of tables

EVERYTHING IS MEANINGLESS.
EVEN THE SENTENCE ABOVE.

Acknowledgments

THANKS TO EVERYONE WORKING AT CERN. CERN is a truly unique and special place. I love how the streets are named by physicists. Without the support from the IT department, I could not log into lxplus, check the twikis and finish my work. CERN user's office also made traveling to Europe a much nicer and easier experience for me.

THANKS TO EVERYONE WORKING ON THE LARGE HADRON COLLIDER. Without a fully functional accerator, there would have been no data for me to study. The LHC performed outstandingly since 2015, and all the valuable data is produced from it.

THANKS TO EVERYONE THE ATLAS COLLABORATION, who has supported this remarkable program and has contributed to every bit of the result in my thesis. Sir Issac Newton said he was standing on the gaint's showlders to see far and deep into the nature. Similarly. I am standing on the ATLAS(member)'s showlders—it's eight stories high so I hope ATLAS doesn't shrug. Without the excellent work on detector design, commisioning, operational works, reconstruction, data processing, performance studies and recommendations, software support, computing support, and analysis discussions and guidance, I could not have completed this thesis. I truly and sincerely thank all

ATLAS members for their contributions.



Introduction

Why do we look for $bb \rightarrow 4b$?

There are two types of analysis in particle physics. The first one is measurement, which yields a observable with an uncertainty. This could either improve our current knowledge, or show some inconsistency. The other type is search, which generally assumes some new physics model and try to justify in data whether the new model is justified in some observables. A successful search turns the subject into a measurement, yet a null search result will set a new limit for a given physics model.

After Run 1 of the LHC, with the existence of the Higgs now firmly established, the focus shifted to searches for physics beyond the Standard Model. In particular, searches for high mass resonances

benefit from the LHC's increase to $\sqrt{s} = 13$ TeV in Run 2. The cross section for a generic gluon-initiated resonance with a mass of 2 TeV increases tenfold in Run 2, making searches for high mass resonances a high priority. The newly discovered Higgs can be used as a tool in these searches. After the discovery, the Higgs boson provides a large swath of unmeasured phase space where new physics could be discovered. Higgs pair production in the Standard Model has a low cross section that requires large datasets (on the order of the LHC's lifetime) for full measurement. However, new physics can modify this cross section, especially through new resonances which decay to two Higgs bosons. Such high mass resonances also produce difficult to recognize final state topologies due to the merging of decay products from high momentum Higgs bosons. A search for Higgs pair production in the $HH \rightarrow b\bar{b}b\bar{b}$ final state was performed with 3.2fb^{-1} collected with ATLAS at $\sqrt{s} = 13$ TeV in 2015. The results are presented in this dissertation with a focus on a dedicated signal region for boosted final states. This signal region uses new techniques for recognizing jet substructure and b -tagging to improve signal acceptance of high mass resonances.

The discovery of the Standard Model (SM) Higgs boson (h)^{1,2} at the Large Hadron Collider (LHC) motivates searches for new physics using the Higgs boson as a probe. In particular, many models predict cross sections for Higgs boson pair production that are significantly greater than the SM prediction. Resonant Higgs boson pair production is predicted by models such as the bulk Randall–Sundrum model^{3,4}, which features spin-2 Kaluza–Klein gravitons, G_{KK}^* , that subsequently decay to a pair of Higgs bosons. Extensions of the Higgs sector, such as two-Higgs-doublet models^{5,6}, propose the existence of a heavy spin-0 scalar that can decay into h pairs. Enhanced non-resonant Higgs boson pair production is predicted by other models, for example those featuring light coloured scalars⁷ or direct $t\bar{t}hh$ vertices^{8,9}.

Previous searches for Higgs boson pair production have all yielded null results. In the $b\bar{b}b\bar{b}$ channel, ATLAS searched for both non-resonant and resonant production in the mass range of 400–3000 GeV using 3.2fb^{-1} of 13 TeV data¹⁰ collected during 2015. CMS searched for the production of resonances

with masses of 750–3000 GeV² using 13 TeV data and with masses 270–1100 GeV with 8 TeV data². Using 8 TeV data, ATLAS has examined the $b\bar{b}b\bar{b}$ ³, $b\bar{b}\gamma\gamma$ ³, $b\bar{b}\tau^+\tau^-$ and $W^+W^-\gamma\gamma$ channels, all of which were combined in Ref.³. CMS has performed searches using 13 TeV data for the $b\bar{b}\tau^+\tau^-$ ⁴ and $b\bar{b}\ell\nu\ell\nu$ ⁵ final states, and used 8 TeV data to search for $b\bar{b}\gamma\gamma$ ⁶ in addition to a search in multilepton and multilepton+photons final states⁷.

The analyses presented in this paper exploit the dominant $h \rightarrow b\bar{b}$ decay mode to search for Higgs boson pair production in both resonant and non-resonant production. Two analyses are presented, which are complementary in their acceptance, each employing a unique technique to reconstruct the Higgs boson. The “resolved” analysis is used for hh systems in which the Higgs bosons have Lorentz boosts low enough that four b -jets can be reconstructed. The “boosted” analysis is used for those hh systems in which the Higgs bosons have higher Lorentz boosts, which prevents the Higgs boson decay products from being resolved in the detector as separate b -jets. Instead, each Higgs boson candidate consists of a single large-radius jet, and b -decays are identified using smaller-radius jets built from charged-particle tracks.

Both analyses were re-optimized with respect to the former ATLAS publication²; an improved algorithm to pair b -jets to Higgs boson candidates is used in the resolved analysis, and in the boosted analysis an additional signal-enriched sample is utilized. The dataset comprises the 2015 and 2016 data, corresponding to 27.5 fb⁻¹ for the resolved analysis and 36.1 fb⁻¹ for the boosted analysis, with the difference due to the trigger selections used. The results are obtained using the resolved analysis for a resonance mass between 260 and 1400 GeV, and the boosted analysis between 800 GeV and 3000 GeV. The main background is multijet production, which is estimated from data; the sub-leading background is $t\bar{t}$, which is estimated using both data and simulations. The two analyses employ orthogonal selections, and a statistical combination is performed in the mass range where they overlap. The final discriminants are the four-jet and dijet mass distributions in the resolved and boosted analyses, respectively. Searches are performed for the following benchmark signals: a spin-2

graviton decaying into Higgs bosons, a scalar resonance decaying into a Higgs boson pair, and SM non-resonant Higgs boson pair production.

This dissertation begins by discussing the status of di-Higgs. Chapter 1 gives an overview of double Higgs production in the Standard Model and beyond. Chapter 2 and 3 present details regarding the Large Hadron Collider and the ATLAS experiment. Chapter 4 provides an overview of object reconstruction in ATLAS, with a focus on Muon Segment Seeding. A brief interlude in Chapter 5 on the ATLAS Muon Data Quality, as this has been a focus of my graduate work.

The rest of the dissertation presents a search for Higgs pair production in the $HH \rightarrow b\bar{b}b\bar{b}$ channel. Chapter 6 presents an overview of physics object selection, where the Higgs pairs are the result of the decay of a heavy resonance. Chapter 7 discusses the background estimation techniques in detail, followed by Chapter 8, Systematics. Chapter 9 presents the results, and Chapter 10 shows the limits between the boosted regime and the resolved regime, which is sensitive to lower mass resonances and non-resonant Higgs pair production. Finally, the work is summarized a conclusion and brief outlook of future Higgs physics with ATLAS.

Knowledge knows no bounds.

Creator

1

Motivation and Theory

1.1 THE STANDARD MODEL AND THE HIGGS BOSON

The Standard Model(SM) ^{1,5,6,7} is a quantum field theory describing the fundamental particles, shown in Figure 1.1. So far, the SM predictions agree extremely well with experimental observations.

In the SM, the Higgs mechanism introduces a complex scalar Higgs field, ϕ , with nonzero vacuum expectation values. Through spontaneous symmetry breaking of the Higgs potential $V(\phi) = -\nu^2\lambda_\nu\phi^\dagger\phi + \lambda_\nu(\phi^\dagger\phi)^2$, W^\pm and Z bosons acquire their masses. This process also predicts an extra scalar, the Higgs boson. The SM Lagrangian containing Higgs couplings, $\mathcal{L}_{\text{Higgs}}$, is shown in Eq 1.1.

$$\mathcal{L}_{\text{Higgs}} = -g_{h\bar{f}f}h\bar{f}f + \partial_\nu V_\mu V^\mu \left(g_{h\nu\nu}h + \frac{g_{hh\nu\nu}}{2}h^2 \right) + \frac{g_{hh}}{2}h^2 + \frac{g_{hhh}}{6}h^3 + \frac{g_{hhhh}}{24}h^4 \quad (1.1)$$

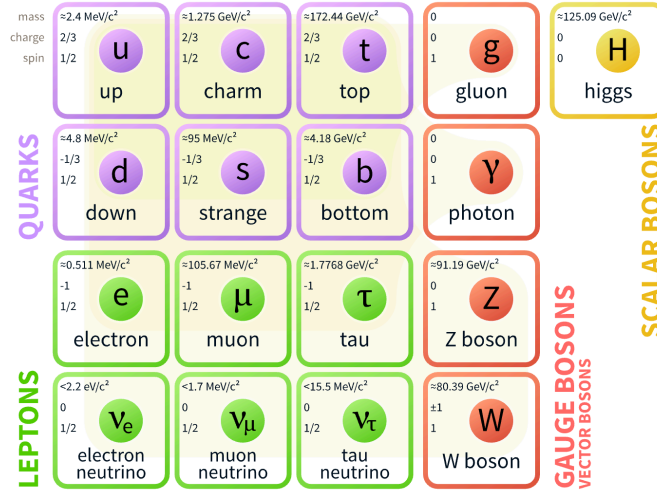


Figure 1.1: Fermions and bosons of the Standard Model and their properties¹, where all the values are measured experimentally.

where

- $v \sim 246 \text{ GeV}$, is the non-zero expectation value of the Higgs field;
- $m_h = \sqrt{2\lambda_\nu} v \sim 125 \text{ GeV}$, is the Higgs mass; this is discovered in 2012^{8,9};
- λ_ν , coefficient for the quartic potential term, is constrained from Higgs mass, to be ~ 0.13 ;
- $V = W^\pm$ or Z , $\delta_W = 1$, $\delta_Z = \frac{1}{2}$;
- $g_{h\bar{f}f} = \frac{m_f}{v}$, is the Higgs to fermion coupling; m_f is the mass of the fermion;
- $g_{hVV} = \frac{2m_V^2}{v}$, is the Higgs to boson coupling; m_V is the mass of the boson;
- $g_{hhVV} = \frac{2m_V^2}{v^2}$, is the Higgs-Higgs to boson-boson coupling;
- $g_{hh} = m_h^2$, is the Higgs mass term;
- $g_{hhh} = \frac{3m_h^2}{v} = 6\lambda_\nu v$, or λ_{hhh} , is the Higgs self-coupling;
- $g_{hhhh} = \frac{3m_h^2}{v^2}$, is the Higgs quartic-coupling.

What's particularly interesting in Eq 1.1 is the $\frac{g_{hhh}}{6}h^3$ term. This coefficient $\frac{g_{hhh}}{6}$, or λ_{hhh} , is also referred as λ_{SM} in this thesis. This term shows one way for two Higgs production within the SM. Double Higgs production is also known as di-Higgs or Higgs pair production.

1.2 STANDARD MODEL DI-HIGGS PRODUCTION

There are two main production modes of di-Higgs at the LHC, shown in Figure 1.2. In the gluon fusion process, di-Higgs are produced through a box or a triangle loop (both mainly of top quarks). Only the triangle loop 1.2b probes the λ_{hhh} . This is showing the off-shell component, where the middle Higgs boson acts as a propagator (off-shell) and the two Higgs bosons in the final state are on-shell. The on-shell component, with two off-shell Higgs bosons in the final state, is strongly disfavored¹. The two diagrams interfere destructively, which makes the overall production rate smaller than what would be expected in the absence of a λ_{hhh} term.

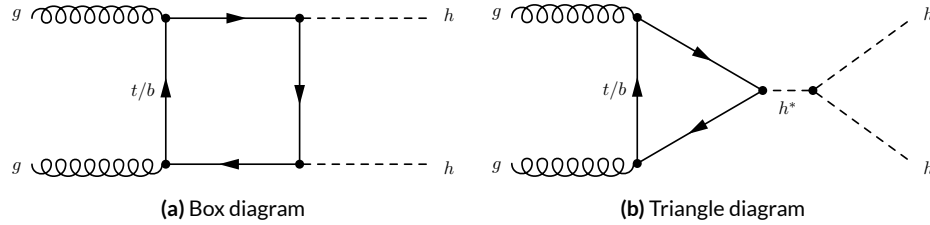


Figure 1.2: Feynman diagrams contributing to di-Higgs production via gluon-gluon fusion, through the Higgs-fermion Yukawa interactions 1.2a the Higgs boson self-coupling 1.2b, at leading order. Only Figure 1.2b probes λ_{hhh} .

Many other different production modes of di-Higgs exist, but gluon-gluon fusion is the dominant one. Figure 1.3¹⁰ compares gluon-gluon fusion, Vector Boson Fusion (VBF), and top-pair, W^\pm , Z and single-top associated di-Higgs production.

The total cross section for SM gluon fusion di-Higgs production¹¹, at the Next to Next Leading Order (NNLO) with top quark mass effects, is $33.49^{+4.3\%}_{-6.0\%} \pm 2.1\% \pm 2.3\%$ fb for p-p collisions at

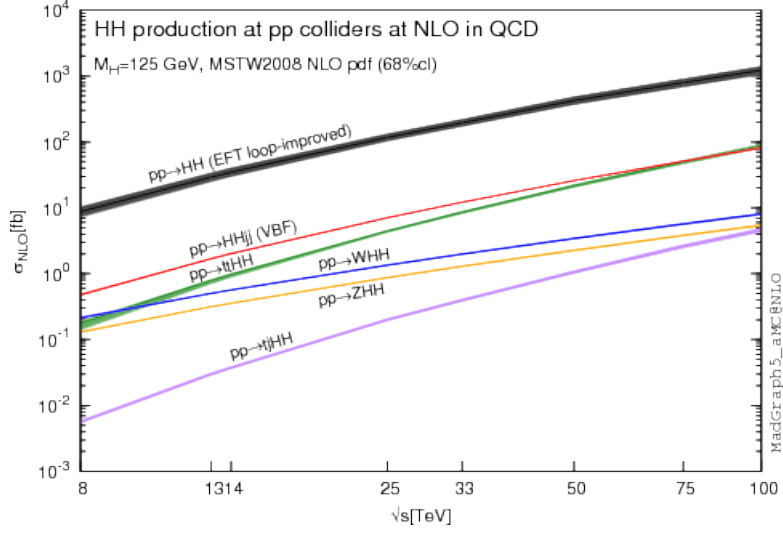


Figure 1.3: Total cross sections (y-axis) at the NLO in QCD for the six largest di-Higgs production channels at p-p colliders at different energy (x-axis). The thickness of the lines corresponds to the scale and PDF uncertainties added linearly. H refers to the SM Higgs.

$\sqrt{s} = 13$ TeV. The cross section for the next dominante production, VBF, is $1.62^{+2.3\%}_{-2.7\%} \pm 2.3\%$ fb. The eistiamted cross section for triple-Higgs production is $0.06332^{+16.1\%}_{-14.1\%} \pm 3.4\%$ fb, which is negeligible. The uncertainties are Scale uncertainty, PDF uncertainty and α_s uncertainty. This means inside 2015 and 2016 $\sqrt{s} = 13$ TeVATLAS data at 36 fb^{-1} , there are only on the order of one thousand SM di-Higgs events.

1.3 BEYOND THE STANDARD MODEL PHYSICS DI-HIGGS PRODUCTION

BSM physics could significantly enhance the production of di-Higgs at the LHC. This is separated into two categories: non-resonant and resonant productions. The non-resonant production generally refers to modifications of the Higgs couplings, either the Higgs self-coupling or the Higgs-top couplings. Resonant production refers to a particle with invariant mass greater than twice the Higgs mass decays directly into two Higgs bosons. The difference also comes from the distribution of the di-Higgs invariant mass at the truth level. In the non-resonant case, the distribution has no

clear peak, whereas in the resonant case, the invariant mass distribution forms a peak with model-dependent width.

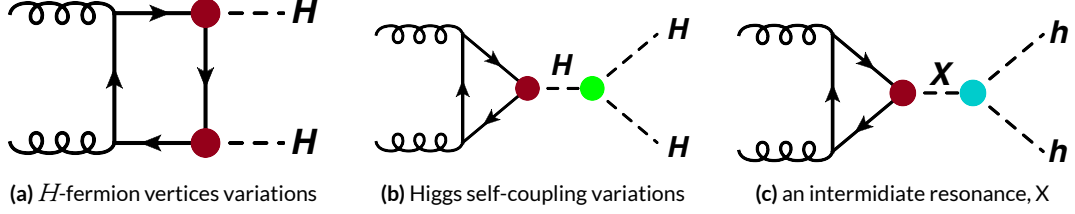


Figure 1.4: BSM Higgs boson pair production: non-resonant production proceeds through changes in the SM Higgs couplings in 1.4a and 1.4b, resonant production proceeds through 1.4c an intermediate resonance, X . H and h both refers to the SM Higgs.

Enhanced non-resonant Higgs boson pair production is predicted by many models. Models featuring direct $t\bar{t}h$ vertices^{3,4} or new light coloured scalars² could change vertices shown as the red dots in Figure 1.4. A direct modification of Higgs self-coupling term in Eq 1.1 to λh^4 , where λ is different from λ_{SM} , is also possible. This is shown as the green dot in Figure 1.4b. The non-resonant di-Higgs enhancement is usually described by $\frac{\lambda}{\lambda_{\text{SM}}}$, which is the cross section ratio between λ and λ_{SM} . Within the SM, from the electroweak measurements, the self coupling term could be constrained to $-14 \leq \frac{\lambda}{\lambda_{\text{SM}}} \leq 17.4$ ¹². Variations of λ have a non-trivial effect on di-Higgs production cross section, shown in Figure 1.5¹⁰.

Resonant Higgs boson pair production is predicted by models such as the bulk Randall–Sundrum model^{2,3}, which features spin-2 Kaluza–Klein gravitons, G_{KK}^* , that subsequently decay to pairs of Higgs bosons. Extensions of the Higgs sector, such as two-Higgs-doublet models^{2,3}, propose the existence of a heavy spin-0 scalar that can decay into h pairs.

The Randall–Sundrum model is a proposed solution to the hierarchy problem that posits a five-dimensional warped spacetime that contains two branes: one where the force of gravity is very

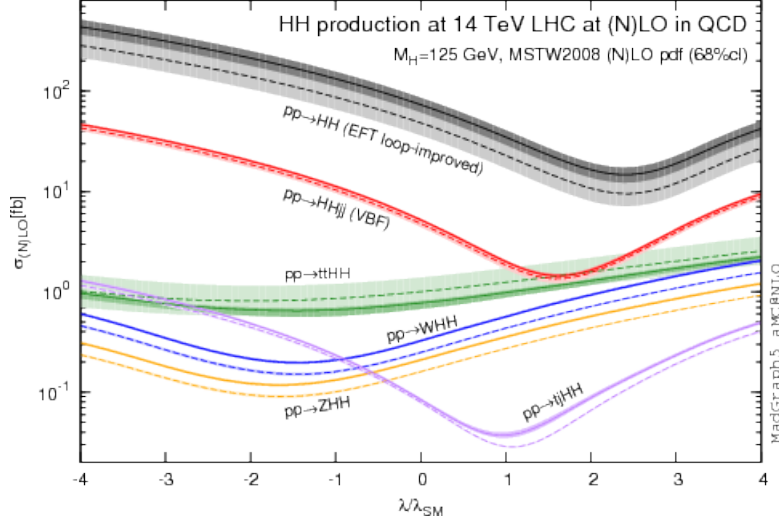


Figure 1.5: Total cross sections (y-axis) at the LO and NLO in QCD for di-Higgs production channels, at the $\sqrt{s} = 14$ TeV LHC as a function of the self-interaction coupling λ (x-axis). The dashed (solid) lines and light- (dark-) colour bands correspond to the LO (NLO) results and to the scale and PDF uncertainties added linearly. The SM values of the cross sections are obtained at $\frac{\lambda}{\lambda_{\text{SM}}} = 1$. H refers to the SM Higgs.

strong and a second brane at the TeV scale corresponding to the known Standard Model sector². In the theory, the branes are weakly coupled and the graviton probability function drops exponentially going from the gravity brane to the SM brane, rendering gravity weak on the SM brane. The experimental consequence of this theory is a tower of widely spaced (in mass) Kaluza-Klein graviton resonances. In theories where the fermions are localized to the SM brane, production of gravitons from fermion pairs is suppressed and the primary mode of production is gluon fusion³. These gravitons have a substantial branching fraction to Higgs pairs, ranging from 6.43% for gravitons with a mass of 500 GeV to 7.66% at 3 TeV. Figure ?? shows the branching ratios of the spin-2 Randall Sundrum graviton (RSG) as a function of its mass. The predominant decays are to $t\bar{t}$ above the mass threshold for that channel.

Randall-Sundrum models have two free parameters - the mass of the graviton and a curvature parameter k . Typically, rather than k , the theory is parameterized using $c \equiv k/\bar{M}_{\text{pl}}$, where \bar{M}_{pl} is

the reduced Planck mass. The cross section for production of the RSG decreases as a function of mass and is strongly dependent on the gluon PDF. The increase in center of mass energy from 8 to 13 TeV in LHC Run 2 greatly increases the cross section at higher mass. Figure ?? shows the cross section as a function of graviton mass at $\sqrt{s} = 13$ TeV for RSG models with $c = 1.0$ and $c = 2.0$.

Another interesting feature of the theory is that the width of the graviton increases with both c and mass. Figure ?? shows the graviton width for both $c = 1.0$ and $c = 2.0$ as a function of mass. In $c = 1.0$, the width starts at 8.365 GeV for a mass of 300 GeV and increases to 187.2 GeV at a mass of 3 TeV. Similarly, with $c = 2.0$, the width starts at 33.46 GeV for $m_G = 300$ GeV and increases to 748.8 GeV at a mass of 3 TeV.

In Two Higgs Doublet Models (2HDM), a second complex scalar doublet is added to the Standard Model^{2,3}. In this case, all four degrees of freedom in the second doublet correspond to new particles, meaning that there are five total scalars from the two Higgs doublets - h (light CP-even Higgs), H (heavy CP-even Higgs), A (heavy CP-odd Higgs), and H^\pm (charged Higgs). The model is parameterized by two main parameters. The first, $\tan \beta \equiv \frac{v_2}{v_1}$, is the ratio of the vacuum expectation values of the two Higgs doublets (where v_1 corresponds to the v in the SM Higgs model described above). The second parameter is α , a mixing angle between the heavy and light Higgs fields. Models are also often parameterized with $\cos(\beta - \alpha)$ rather than α directly. The limit where $\cos(\beta - \alpha) = 0$ is called the alignment limit, and in this limit the light Higgs h has the same couplings as a Standard Model Higgs. Measurements of the Higgs boson have put constraints on these two parameters, but near the alignment limit there is still much unprobed phase space depending on the exact models and values of $\tan \beta$ being considered².

2HDM models are usually separated into two main types - Type I and Type II. In Type I models, the charged fermions only couple to the second Higgs doublet, leading to a fermiophobic light

Higgs. In Type II models, up-type quarks couple to the first doublet while down-type quarks couple to the second doublet. One specific realization of a Type II 2HDM is the Minimal Supersymmetric Standard Model (MSSM).

Resonant di-Higgs production in 2HDM models can proceed through decays of the heavy CP-even Higgs $H \rightarrow b\bar{b}$. The branching ratio for $H \rightarrow b\bar{b}$ depends on the model type as well as the values of $\tan\beta$ and $\cos\beta - \alpha$. Figure ?? shows the branching ratios as a function of the mass of the heavy scalar H for both Type I and Type II models. Depending on the type of model, $b\bar{b}$ can be a substantial fraction of the decays of H .

With the increased center of mass collision energy, the production cross section grows, particularly for heavy particles above TeV.

1.4 DI-HIGGS DECAY

Di-Higgs decay is the combination of single Higgs decays.

1.5 LHC PREVIOUS SEARCH RESULTS

Previous searches for Higgs boson pair production have all yielded null results. In the $b\bar{b}b\bar{b}$ channel, ATLAS searched for both non-resonant and resonant production in the mass range of 400–3000 GeV using 3.2 fb^{-1} of 13 TeV data[?] collected during 2015. CMS searched for the production of resonances with masses of 750–3000 GeV using 13 TeV data[?] and with masses 270–1100 GeV with 8 TeV data[?]. Using 8 TeV data, ATLAS has examined the $b\bar{b}b\bar{b}$ [?], $b\bar{b}\gamma\gamma$ [?], $b\bar{b}\tau^+\tau^-$ and $W^+W^-\gamma\gamma$ channels, all of which were combined in Ref.[?]. CMS has performed searches using 13 TeV data for the $b\bar{b}\tau^+\tau^-$ [?] and $b\bar{b}\ell\nu\ell\nu$ [?] final states, and used 8 TeV data to search for $b\bar{b}\gamma\gamma$ [?] in addition to a search in multilepton and multilepton+photons final states[?].

2

Conclusion

Di-Higgs search has a short history, but will have a long future. This thesis presents a search for both resonant and non-resonant production of pairs of Standard Model Higgs bosons has been carried out in the dominant $b\bar{b}b\bar{b}$ channel, using $27.5\text{--}36.1\text{ fb}^{-1}$ of LHC pp collision data at $\sqrt{s} = 13\text{ TeV}$ collected by ATLAS in 2015 and 2016. The search sensitivity of this analysis exceeds that of the previous analysis of the $\sqrt{s} = 13\text{ TeV}$ 2015 dataset² for non-resonant signal and also across the entire mass range of 260-3000 GeV for the resonance search, with significantly improvement in the high mass resonance sensitivities. The resolved analysis has each $b \rightarrow b\bar{b}$ reconstructed as two separate b -tagged jets, and the boosted analysis has each $b \rightarrow b\bar{b}$ reconstructed as a single large-radius jet associated with at least one small-radius b -tagged track-jet. The estimated background consists mainly of multi-jet and $t\bar{t}$ events.

No significant excess is observed in the data. The largest deviation from the background-only hypothesis is observed for narrow signal models at a mass of 280 GeV in the resolved analysis, with a global significance of 2.3σ . This excess could be a trigger-turn on combined with kinematic selection effect and might not last with more data. Upper limits on the production cross section times branching ratio to the $b\bar{b}b\bar{b}$ final state are set for a narrow-width scalar and for spin-2 resonances. The 95% CL upper limit on the non-resonant production is 147 fb, which corresponds to 13.0 times the SM expectation.

Future improvement with the rest of $\sqrt{s} = 13$ TeV Run II could come from improving b -tagging, especially in the high p_T region. Advanced trigger technologies and selections will increase the data rate, and better jet energy and mass resolution will increase the purity in selection. With the larger dataset and improvements in physics performance, it is possible to reach twice as the current sensitivity of resonance searches. For non-resonance searches, an order of 10 times the SM expectation is more sensible at the end of Run II.

For longer term perspectives, di-Higgs measurements will continue to be one of the most important analysis that help constraining our understanding of physics beyond the Standard Model. Given the current status, it is possible that in fifteen to twenty years there will be no new discovery, and the experiments at the LHC will be able to constrain the Higgs self-coupling within unity.

As humans, we have a limited life. However, physics, as well as the understanding of the universe, is an endless journey. I sincerely hope that my biased prediction of the future of Higgs physics will be wrong, but nevertheless I am deeply honored to be a small part of this odyssey towards Veritas.

References

- [1] C. Patrignani et al. Review of Particle Physics. *Chin. Phys.*, C40(10):100001, 2016. doi: 10.1088/1674-1137/40/10/100001.
- [2] Graham D. Kribs and Adam Martin. Enhanced di-higgs production through light colored scalars. *Phys. Rev. D*, 86:095023, 2012. doi: 10.1103/PhysRevD.86.095023.
- [3] R. Gröber and M. Mühlleitner. Composite Higgs boson pair production at the LHC. *JHEP*, 06:020, 2011. doi: 10.1007/JHEP06(2011)020.
- [4] Roberto Contino et al. Anomalous couplings in double Higgs production. *JHEP*, 08:154, 2012. doi: 10.1007/JHEP08(2012)154.
- [5] David Griffiths. *Introduction to elementary particles*. 2008.
- [6] Christopher G. Tully. *Elementary particle physics in a nutshell*. 2011.
- [7] Matthew D. Schwartz. *Quantum Field Theory and the Standard Model*. Cambridge University Press, 2014. ISBN 1107034736, 9781107034730.
- [8] ATLAS Collaboration. Observation of a new particle in the search for the Standard Model Higgs boson with the ATLAS detector at the LHC. *Phys. Lett. B*, 716:1, 2012. doi: 10.1016/j.physletb.2012.08.020.
- [9] CMS Collaboration. Observation of a new boson at a mass of 125 GeV with the CMS experiment at the LHC. *Phys. Lett. B*, 716:30, 2012. doi: 10.1016/j.physletb.2012.08.021.
- [10] R. Frederix, S. Frixione, V. Hirschi, F. Maltoni, O. Mattelaer, P. Torrielli, E. Vryonidou, and M. Zaro. Higgs pair production at the LHC with NLO and parton-shower effects. *Phys. Lett.*, B732:142–149, 2014. doi: 10.1016/j.physletb.2014.03.026.
- [11] D. de Florian et al. Handbook of LHC Higgs Cross Sections: 4. Deciphering the Nature of the Higgs Sector. 2016. doi: 10.23731/CYRM-2017-002.

- [12] Graham D. Kribs, Andreas Maier, Heidi Rzehak, Michael Spannowsky, and Philip Waite. Electroweak oblique parameters as a probe of the trilinear Higgs boson self-interaction. *Phys. Rev.*, D95(9):093004, 2017. doi: 10.1103/PhysRevD.95.093004.